PALAIOS
Emphasizing the impact of life on Earth's history

PALAIOS, 2013, v. 28, p. 438–451
Research Article
DOI: 10.2110/palo.2012.p12-111r

CRYPTIC DIAGENETIC CHANGES IN QUATERNARY ARAGONITIC SHELLS: A TEXTURAL, CRYSTALLOGRAPHIC, AND TRACE-ELEMENT STUDY ON *AMIANTIS PURPURATA* (BIVALVIA) FROM PATAGONIA, ARGENTINA

M. SOL BAYER,[1]* FERNANDO COLOMBO,[1] NATALIA S. DE VINCENTIS,[2] GONZALO A. DUARTE,[2] RAÚL BOLMARO,[2] and SANDRA GORDILLO[1]

[1]*Centro de Investigaciones en Ciencias de la Tierra, Universidad Nacional de Córdoba (CICTERRA-CONICET-UNC), Av. Vélez Sarsfield 1611, Córdoba, X5016GCA, Argentina, sol.bayer@conicet.gov.ar, fosfatos@yahoo.com.ar, gordillosan@yahoo.es;* [2]*Instituto de Física de Rosario, Universidad Nacional de Rosario-CONICET, Bv. 27 de Febrero 210 bis, Rosario 2000, Argentina, devicentis@ifir-conicet.gov.ar, gonzaloarielduarte@yahoo.com.ar, bolmaro@ifir.edu.ar*

ABSTRACT

Modern to Pleistocene *Amiantis purpurata* shells collected in Bahía San Antonio (Patagonia, Argentina) were studied by X-ray diffraction (XRD), optical and electron microscopy, electron microprobe analyses, and microindentation, in order to characterize early diagenetic changes and mechanical resistance. The sole crystalline phase is twinned aragonite showing pseudohexagonal symmetry. The regularity of the crystallographic texture decreases in older samples, but average crystallite size does not increase. The microstructure, which is dominantly crossed lamellar, is progressively replaced by a more randomly oriented grain aggregate. Compositional profiles across the shell show gradients in Sr, Na, S, and Cl, whereas Mg and P are more evenly distributed. Each shell layer has a distinct chemical signature. A marked decrease in the concentration of all of these elements, along with flattening of profiles, is evident as age increases. Vickers microhardness is lowest in modern specimens, showing at the same time the least chipped regions; older shells become harder and more fragile. All of these changes are attributed to postdepositional modifications by dissolution-recrystallization processes mediated by a thin film of water in a vadose environment. Microstructural adjustments are more sluggish than chemical modifications produced by diagenetic processes, whereas microhardness rapidly reaches high values, probably due to the early degradation of organic compounds from the shell. Our study shows that aragonitic shells that retain their primary mineralogical composition have undergone subtle chemical and microstructural changes. A very small amount of calcite was produced during grinding for XRD. Care should therefore be taken when seeking calcite as evidence of diagenetic changes.

INTRODUCTION

Bivalve mollusks have often been used in comparative taphonomic studies because of their excellent potential for preservation (Chave, 1964; Raup and Stanley, 1978; Jablonski et al., 2003). However, their resistant hard parts are subject to physical, chemical, and biological agents or processes that can destroy these shells before and after burial (e.g., Lawrence, 1968).

Bivalve shells are predominately composed of calcium carbonate (calcite, aragonite, or both in variable proportions), as well as organic polymers (Hare and Abelson, 1965; Rhoads and Lutz, 1980). As in other biomineralized exoskeletons, the orientation and growth of $CaCO_3$ crystals are strongly controlled by the organic matrices (which constitute about 1–5 wt% of the shell) forming compartments in which mineralization takes place. Most of the organic components are intercrystalline, with a smaller portion located within the crystal structure of calcium carbonate. This mixture, on a very fine scale of organic and bioprecipitated $CaCO_3$, modifies diagenetic processes and patterns in comparison with nonbiogenic mineral features (Perrin and Smith, 2007).

Mollusk shells can be considered inorganic-organic biocomposites, with excellent mechanical performance compared to nonbiogenic material (Chateigner et al., 2010). Even though aragonite provides high mechanical strength to the valve (Chateigner et al., 2000), under the environmental conditions found on the Earth's surface, this phase is metastable, and is more susceptible to dissolution and recrystallization than calcite. In other words, during diagenesis, the alteration of aragonite skeletons commonly results in mineralogical and structural changes, as well as compression and postdepositional cementation (Brand, 1989). For this reason, aragonitic fossils are usually poorly preserved in the geological record (Spaeth et al., 1971; Powell and Kowalewski, 2002; Jablonski et al., 2003; Cherns et al., 2011). One exception is for the Cenozoic A-seas (aragonitic seas), in which a positive bias favoring aragonitic bivalves is recognized (De Renzi and Ros, 2002). Some examples of preserved aragonite remains (older than Pleistocene) include bivalves from the Eocene of the Anglo-Paris Basin (Jefferies, 1961), the Jurassic of Scotland (Sandberg and Hudson, 1983), the Late Cretaceous of Antarctica (Pirrie and Marshal, 1990), the Late Cretaceous and Paleogene of North America (Dettmann and Lohmann, 2000; Fan and Dettmann, 2010), and from the Eocene of the UK (Purton et al., 1999).

This relative instability of aragonite when exposed to diagenesis introduces a bias in the fossil record, affecting its quality for paleoecological and paleobiological studies (Fernández López, 2000; Cherns and Wright, 2009; Allison and Bottjer, 2011). In addition, some techniques widely applied in carbonate geochemistry, such as isotopic analyses to determine age, paleotemperatures or stratigraphic correlation, and paleoenvironmental and paleoecological studies based on the trace-element and isotopic content of carbonate skeletal remains, assume that the valves behaved as a closed system from the time of deposition.

The detection of subtle postdepositional changes therefore becomes of utmost importance, especially in fossils that appear to retain their primary mineralogy when conventional screening techniques (such as X-ray diffraction) are used. In this article we describe the chemical (trace element), textural, and physical-mechanical transformation that has taken place in shells of the *Amiantis purpurata* venerid, an aragonitic bivalve, during early diagenesis in a period of time that exceeds 100,000 years (from the Late Pleistocene up to the present day).

Amiantis purpurata is found in the fossil record from the Eocene up to today (Forbes, 1856; da Silva Forti, 1969; Addicott, 1973; Angulo et al., 1978; Tantanasiriwong, 1979; Nilsen, 1987; Frassinetti and Covacevich, 1993; Del Rio, 2000; Lézine et al., 2002, among others), and it is currently distributed from the coasts of Espirito Santo (Brazil) to the Golfo San Matías (Patagonia, Argentina). The latter houses the

* Corresponding author.
Published Online: August 2013

 0883-1351/13/0028-0438/$3.00

TABLE 1—Analytical conditions for electron microprobe analyses.

Element	Crystal	Line	Time (peak)	Time (background)*	Standard	Average detection limit¶
Na	TAP	*Kα*	20 s	10 s	albite	75 ppm
Mg	TAP	*Kα*	30 s	15 s	synthetic MgO	50 ppm
P	PETJ	*Kα*	30 s	15 s	fluorapatite	110 ppm
S	PETJ	*Kα*	30 s	15 s	celestite	160 ppm
Cl	PETJ	*Kα*	30 s	15 s	sodalite	70 ppm
K	PETJ	*Kα*	30 s	15 s	orthoclase	60 ppm
Mn	LIF	*Kα*	30 s	15 s	rhodonite	180 ppm
Fe	LIF	*Kα*	30 s	15 s	fayalite	180 ppm
Sr	PETJ	*Lα*	30 s	15 s	celestite	200 ppm
Ba	PETJ	*Lα*	30 s	15 s	sanbornite	180 ppm
Pb	PETJ	*Mα*	30 s	15 s	crocoite	240 ppm

* Counting time at each background position.

¶ Expressed as twice the value calculated based on counting statistics.

largest and southernmost population of this species (Morsán, 2000, 2003; Navarte et al., 2007). The advantage of considering the same species from different outcrops of the same region is the elimination of interspecific variations associated with intrinsic factors (shell microstructure) and different environmental conditions that can occur when comparing shells of the same species collected from different regions. This is because environmental conditions can influence the amount of shell damage and completeness (Meldahl and Flessa, 1990; Feige and Fürsich, 1991; Cutler, 1995; Pandolfi and Greenstein, 1997). Also, shell size, shape, microarchitecture, and mineralogy are important factors in skeletal durability (Chave, 1964; Wainwright, 1969; Glover and Kidwell, 1993). These factors are related to the intrinsic characteristics of taxa, which lead to differential behavior under environmental effects (Boretto et al., 2013). This study minimizes bias by considering the same species from different outcrops of the same region.

SAMPLES AND EXPERIMENTAL METHODS

Samples

Specimens were collected from Bahía San Antonio (San Antonio Bay), located in the north of Golfo San Matías (40°49′S; 64°50′W), Patagonia, Argentina. Pleistocene and Holocene outcrops, as well as modern deposits, are found along the coasts of the gulf (Feruglio, 1950; Fidalgo and Ricci, 1970; Angulo et al., 1978; Rutter et al., 1989; Pastorino, 1989, 2000). In this area, Quaternary marine units are represented by recent beaches, the Pleistocene Baliza San Matías Formation, and the Holocene San Antonio Formation. These outcrops and their faunal composition have been considered by several different authors (Feruglio, 1950; Angulo et al., 1978; Rutter et al., 1989, 1990; and Pastorino, 2000, among others); Feruglio (1950) was the first who noted the presence of *Amiantis purpurata*, among other species of mollusks, during the Quaternary period.

Sediments in the study area are unconsolidated or poorly consolidated, with no evidence of having been subject to significant burial diagenesis. Sandy, fine-grained gravel characterizes Pleistocene and Holocene outcrops. Complete shells and shell fragments characterize only the upper area of the modern beach, while the intertidal area is characterized by medium to fine sand (Fucks et al., 2012).

Both fossil and modern valves exhibit a high degree of abrasion but also a high level of preservation of the original skeletal microstructure characteristic of *A. purpurata.* Preliminary work, including a taphonomic study of valves from Bahía San Antonio, reveals that inner layers were exposed or poorly defined outer layers, thus implying that many of the shells are abraded (Bayer et al., 2010). Agents that work on *A. purpurata*'s remains (fossil and modern specimens), such as water, wind, rocks and other remains, and their intensity during the biostratinomy process, appear to be almost uniform through time.

Five shells from Pleistocene outcrops (>230,000–91,000 B.P.; Rutter et al., 1989, 1990) and five from Holocene sections (5,290 ± 39, 5,648 ± 40 B.P.; Favier Dubois, 2009), together with a few modern valves, were examined. Some of these last specimens still had their ligament, thus showing that their death occurred a short time before being collected. The study shells of the same ontogenic age were selected to allow for meaningful analytical comparison.

Scanning Electron Microscopy (SEM), Electron Microprobe Analyses (EPMA) and Optical Microscopy

Thin sections of standard thickness (about 30 μm) were prepared by sectioning the valves parallel to the growth direction, and examined using optical microscopy with polarized light. A JEOL JXA-8230 electron microprobe located at LAMARX (Facultad de Matemática, Astronomía y Física, Universidad Nacional de Córdoba) was used for quantitative analyses using wavelength-dispersive X-ray spectroscopy. Analyses were performed on mirror-polished and carbon-coated samples (the same thin sections that had been previously examined by optical microscopy) along lines approximately perpendicular to the section line, from the internal to the external side of the valves. An accelerating potential of 15 kV, a current of 20 nA, and an analytical spot diameter of 10 μm were used in order to minimize sample damage. A fixed amount of CO_2 (44.0 wt%), along with the measured Ca content, were included in the ZAF matrix-correction routine. Sodium was measured first and for a shorter counting time, as a very marked decrease (to about 50% of the original concentration) was observed after the shell had been exposed for ~4 minutes to a stationary electron beam. An element was considered to be present when its concentration exceeded at least twice the detection limit calculated on the basis of counting statistics. More details on analytical conditions appear in Table 1. Element-distribution maps of Sr were obtained at 15 kV and 50 nA, with a step size of 2 μm and a dwell time of 50 ms on each point. Unpolished shell fragments were coated with carbon and examined using scanning electron microscopy with the same electron microprobe.

X-Ray Diffraction (XRD)

Shell fragments were cut from equivalent sections of different valves. The shell surfaces were deteriorated but not deeper than 300 to 400 μm, beyond which all of them showed enough integrity to allow careful polishing. Valves used for textural studies by XRD were mounted in epoxy and then polished using standard polishing micrography techniques, grinding the samples on a face tangential to the external surface. Polishing was finished with a suspension of Al_2O_3 (0.5 and 0.03 μm) on a polishing cloth.

X-ray diffraction experiments were performed on a PANalytical MPD diffractometer equipped with a Cu tube ($K\alpha_{1,2}$ radiation), parallel

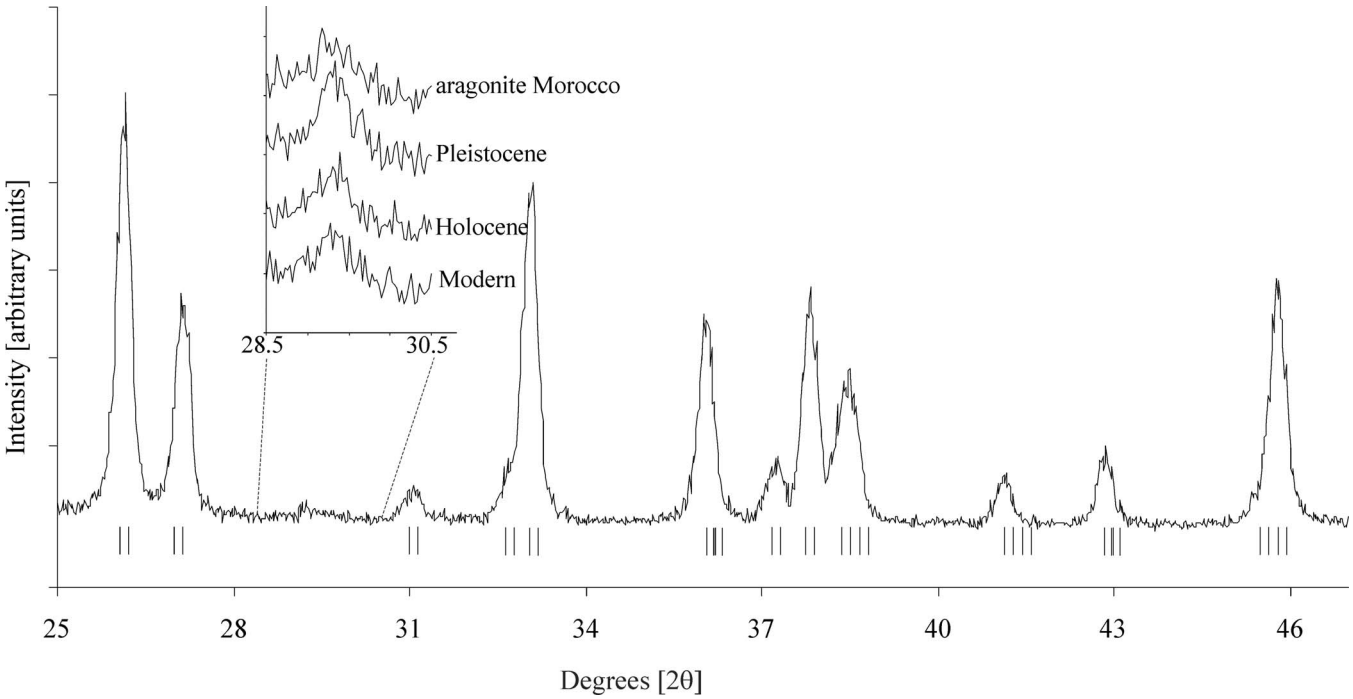

FIGURE 1—X-ray diagram of a Pleistocene shell, measured at a speed of 0.7 s per step. Vertical bars indicate the position of the Bragg reflections for aragonite. Note that peaks are wide, indicating small crystallite size and/or strain. Aragonite has no reflections around 29.5° (2θ), where a small peak is barely visible. Inset: X-ray diagrams taken with a count time of 10 s per step, clearly showing a peak (attributed to calcite) that has about the same intensity regardless of the valve age. The same peak appears in a sample of inorganic aragonite coming from Morocco; calcite is interpreted to have formed during sample grinding.

beam array by virtue of an X-ray lens and parallel beam Soller slits, and flat graphite monochromator in the outgoing beam. Powder diffractograms were taken for $2\theta = 20°–55°$ using 0.02° (2θ) steps and $\Delta t = 1$ s.

Textures were characterized by measuring incomplete (002), (012), (021), (111), and (221) pole figures (corrected for background and defocusing by using a randomly oriented aragonite sample), by the determination of Orientation Distribution Functions (ODF), and by pole figure recalculation for consistency checking and for easing the interpretation of the microstructure orientation with respect to the samples axes. Samples were oriented so that the growth direction is the vertical axis *N* of the pole figures, and the plane tangent to the shell at the beam location has its normal in the center of the pole figures. The analysis was performed by WXpopLA, a current Windows XP compatible version of the popLA package (Kallend et al., 1991). Pole figures are normalized into distribution density units (or m.r.d. for multiple of random distribution), which depend only on orientation. In such units, a specimen without any preferred orientation exhibits 1 m.r.d. homogeneous level in all pole figures, while a textured specimen shows density minima and maxima.

Six additional samples were powdered in an agate mortar for powder XRD, to identify the mineralogy and the crystallite (domains that scatter X-rays coherently) size, using a PANalytical X'PERT diffractometer (housed at the Instituto de Investigaciones en Físico-Química de Córdoba, Universidad Nacional de Córdoba) and Cu$K\alpha_{1,2}$ radiation obtained at 40 kV and 40 mA. Samples were crushed by hand under ethanol, for a period of ~4 minutes. Rietveld refinements for weight quantification were performed using FULLProf software (Roisnel and Rodríguez-Carvajal, 2007) with the structures published by Borodin et al. (1979) and Pokroy et al. (2007). Refined parameters include background, scale, profile parameters, unit cell, preferential orientation, and overall atomic displacement parameter. Atomic positions were not refined.

Microindentation

After texture data collection, the polished samples were used for microindentation characterization by using a Shimadzu HMV-2 microdurometer (Instituto de Fisica Rosario, Universidad Nacional de Rosario). Because of the high sensitivity of the shell fracture strength to the water content, and the possible time dependence of the crack evolution, the measurements were taken using two main precautions: the samples were kept in a moisture-free stable environment for at least 2 weeks before measuring, and the area determinations were made immediately after the indentations. The microindents were performed at distances that guaranteed no interaction between the regions of elastic or plastic deformation or fracture. After hardness measurements, the indentation regions were immediately photographed with an optical microscope. Fractured areas were calculated by using image analysis software (Optimas 5) and were calibrated by simultaneously measuring micrometric rules.

Previous experience with this technique and with the same species (Duarte et al., 2008) led to the selection of two loads which would produce a measurable indentation size while avoiding large scaling or fracture of samples due to excessive loading: 0.49 N and 1.96 N.

RESULTS

Mineralogy

The main phase detected by X-ray diffraction was aragonite, orthorhombic (space group *Pmcn*) $CaCO_3$ (Fig. 1). Traces of calcite (about 0.4 wt%, calculated using the Rietveld method), the trigonal (space group R-3c) polymorph of $CaCO_3$, were apparent in scans using a 10-second counting time, but these likely formed during the grinding process (Fig. 1).

Microstructures

The dominant microstructure in the *Amiantis purpurata* shells is crossed lamellar, as mentioned first by Do Campo (1991) and then analyzed in detail by Bolmaro (2005). As described by Kennedy et al. (1969), crossed-lamellar microstructure is characterized by interdigitated first-order lamellae, extending approximately normal to the shell

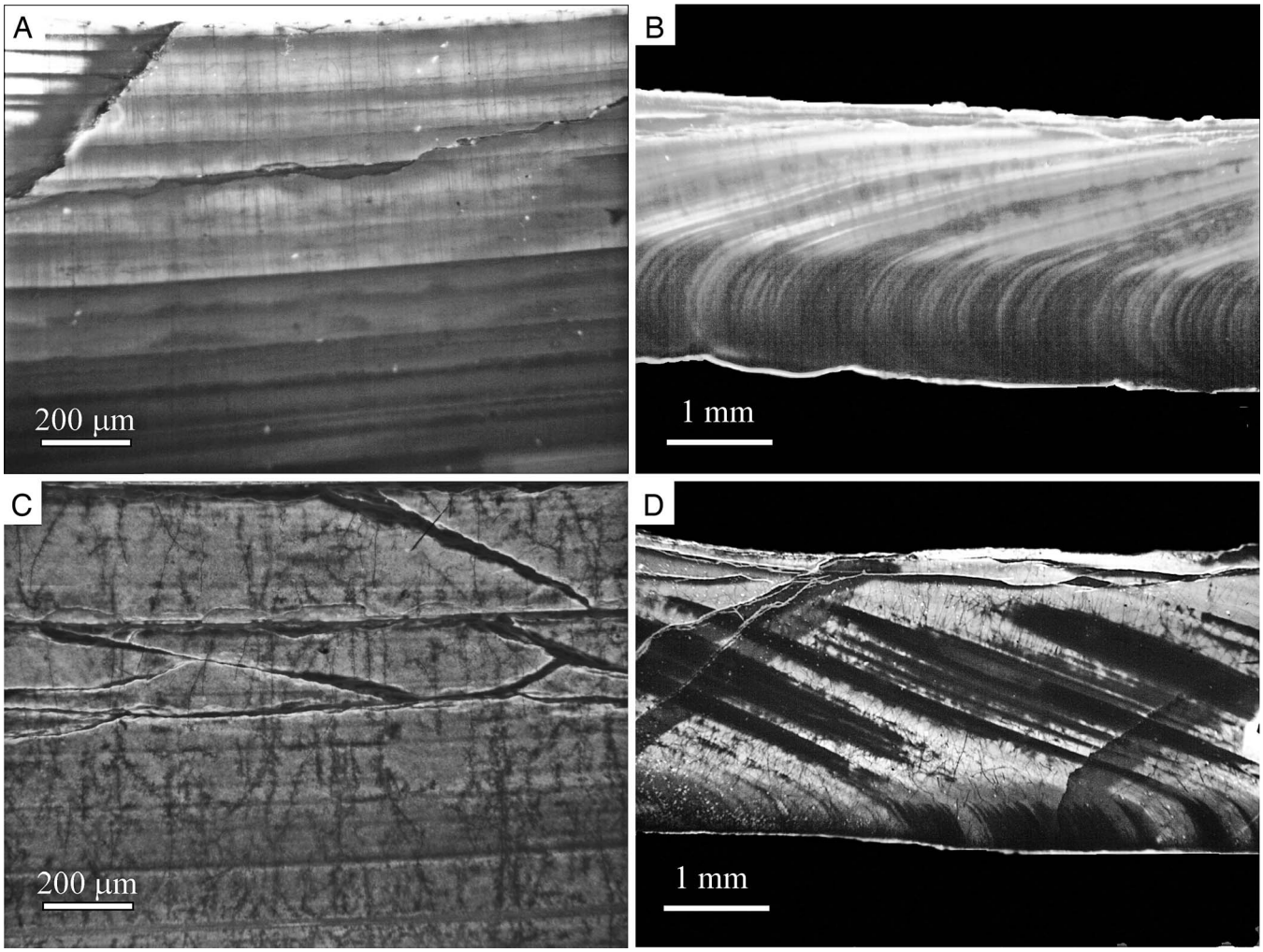

FIGURE 2—Photomicrographs of *Amiantis purpurata* shells (polarized light, crossed polars except for A). In all of the pictures, the inner shell surface is upward. A) Detail of the inner layer of a modern shell, showing parallel bands with shade gradation. B) The same shell, but showing the intermediate layer with inclined bands, and the outer layer, where these bands become almost normal to the surface. In this picture, taken closer to the distal margin of the shell than picture A, the inner layer is not present. C) Holocene shell. Banding is continuous and well preserved, but the shade gradation is lost. D) Pleistocene shell, with increased transparency and discontinuous bands.

inner surface; in turn, each of these first-order lamellae is composed of second-order lamellae arranged at right angles to the sides of the first-order lamellae. Between two adjacent first-order lamellae, the second-order lamellae are arranged in opposite directions, defining a chevron pattern.

Sets of first-order lamellae are arranged in bands. In addition to the beak, there are three layers in the shell; in the first (innermost) layer, these bands are almost parallel to the inner surface. In the second (intermediate) layer they form an angle of about 30° with the inner surface. In the third (outermost) layer these bands bend sharply and become almost normal to the outer surface (Figs. 2B, D). Bands display variable shades of brown in polarized transmitted light. Many layers show a pale-brown color that gradually darkens to the point of becoming almost opaque.

The general structure is well preserved even in the Pleistocene sample, although the fine details are lost. While there are still two shades of brown (light and dark), color gradations are obliterated. Growth rings become laterally discontinuous and transparency is increased (Fig. 2).

Microstructures are clearly seen in SEM images. The modern valve exhibits clear growth bands showing aragonite crystals defining a crossed-lamellar structure (Figs. 3A–C). The Holocene valve displays bands where the crossed-lamellar structure is well preserved, and others where it is mostly obliterated, and is replaced by granular crystals (Figs. 3D–F). A granular, homogeneous texture is dominant in the Pleistocene sample, where no growth ring is visible (Figs. 3G–H) but only isolated domains with crossed-lamellar structure could be discerned (Fig. 3I).

X-ray diffraction peaks are wide, with full width at half maximum (FWHM) values ranging between 0.33° and 0.36° (2θ, Cu$K\alpha_1$), with an outlier value of 0.26°. Average crystallite sizes calculated using the Scherrer equation for the 111 peak (at ~26.2° 2θ) are between 311 and 369 Å (507 Å for the outlier), with no systematic variation among samples of different ages. These values show that crystallite size does not change significantly with the age of the specimen.

The results obtained using XRD indicate that crystallographic textures on the very first few micrometers of depth from the surface are very similar for the modern, Holocene, and Pleistocene valves (m.r.d. values between 4.65 and 5.87). The c axis is inclined with respect to *N*, and crystals have two different orientations (Fig. 4).

Deeper into the samples, it can be seen that the aragonite crystals which define the crossed-lamellar microstructure are twinned, with [001] as a twin axis (Fig. 5). This twin law is the most common for inorganic aragonite, where three crystals bound by the {110} prism form twins of pseudohexagonal symmetry. This appears in XRD textures as a pseudohexagonal pattern defined by the (111) poles. (001) poles are slightly out of the perpendicular direction to the shell external

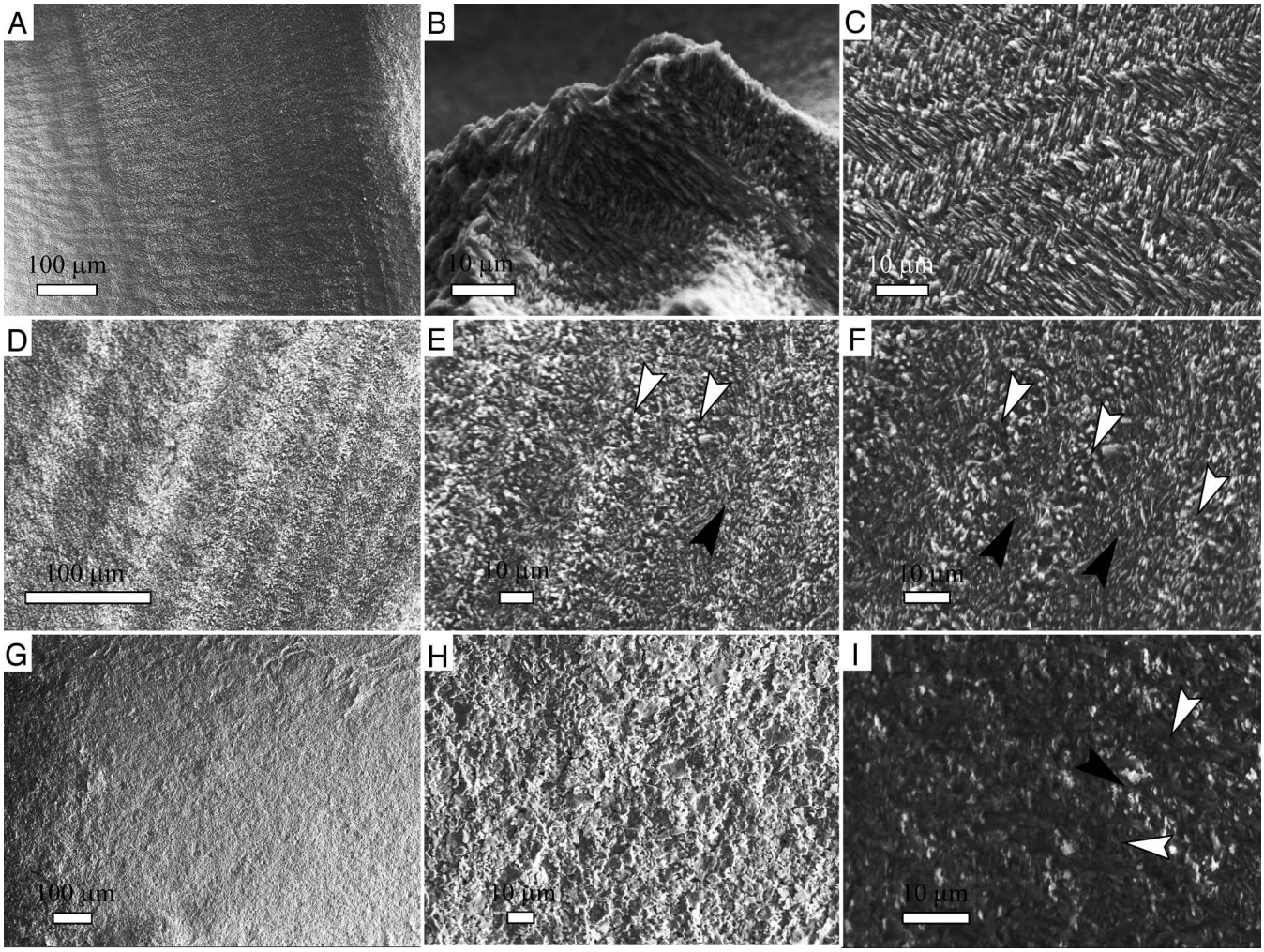

FIGURE 3—SEM images (secondary electron mode) of *Amiantis purpurata* shells. A) General view of a modern shell, where growth bands can be clearly seen. B–C) Details of A, showing platy aragonite crystals defining a crossed-lamellar microstructure. D) General view of a Holocene shell. Growth bands can still be observed. E–F) Detail of D. Some bands (marked with white arrows) have been replaced by a granular aggregate of aragonite crystals, whereas others (black arrows) still display the crossed-lamellar microstructure. G) View of a Pleistocene shell. No growth bands can be discerned. H) Detail of H, showing a homogeneous aggregate of equant aragonite crystals. I) Another sector of the Pleistocene shell, showing a mixture of biogenic platy crystals (white arrows) with equant grains of aragonite of diagenetic origin (black arrow).

surface (15°–20°), but unlike the outer layer, there is a single orientation for the c axis. This arrangement has already been reported for the internal layers of other modern valves (Bolmaro, 2005; Duarte et al., 2008; Chateigner et al., 2010).

All three examined samples display the same crystallographic texture. The regularity of the texture remains approximately constant in the outer layer, regardless of the age. In the inner layers that show crossed-lamellar microstructures, it is noteworthy that the twinning pattern is slightly less well defined in the Holocene sample compared to the modern valve, but the c axes of aragonite crystals are more strongly oriented (78.7 versus 95.2 m.r.d., respectively). The Pleistocene sample shows a marked decrease in the regularity of the texture, with both disorientation of c axes (31.8 m.r.d) and blurring of the twinning pattern.

However, when observed in detail at the same depth or in the same layer, textural pattern shows intraspecific variations. There are also variations in texture between valves from the same organism, i.e., variations in texture between the right and left valves (Fig. 6).

Chemical Composition of the Valves

Three valves were chosen for the study of chemical composition and possible age-related variations in minor element concentrations. In spite of the higher detection limits (about 100 times more) of other techniques such as optical emission or mass spectroscopy, electron microprobe was chosen as a method of analysis because of its better spatial resolution, which enables quantification of chemical changes occurring in points separated by a few µm. Given the large variations in concentrations related to shell age and position of the analysis, average values are meaningless. The whole dataset can be obtained from the online Supplementary Data[1].

Sodium is the most abundant cation after Ca, with up to 0.74 wt% NaO. High Na concentrations comparable to these have been reported previously (e.g., Busenberg and Plummer, 1985; Dalbeck et al., 2006). The Na/Cl molar ratio well above 1 indicates that Na is not (only) present as submicrometric inclusions of halite (NaCl).

Among the divalent trace elements, Sr is invariably above the detection limit (0.05 wt% SrO), and is the element that reaches the highest concentrations (up to 0.53 wt% SrO). This selective incorporation is related to the similarity of their ionic radii (1.18 Å for Ca and 1.31 Å for Sr, both for ninefold coordination, according to Shannon, 1976). The mechanism of Na uptake in the shell is still a matter of debate (see Dalbeck et al., 2006 and Okumura and Kitano, 1986), but in aragonite the ionic radium of ninefold coordinated Na (1.24 Å, Shannon, 1976) is probably a very influential factor as well.

[1] palaios.ku.edu

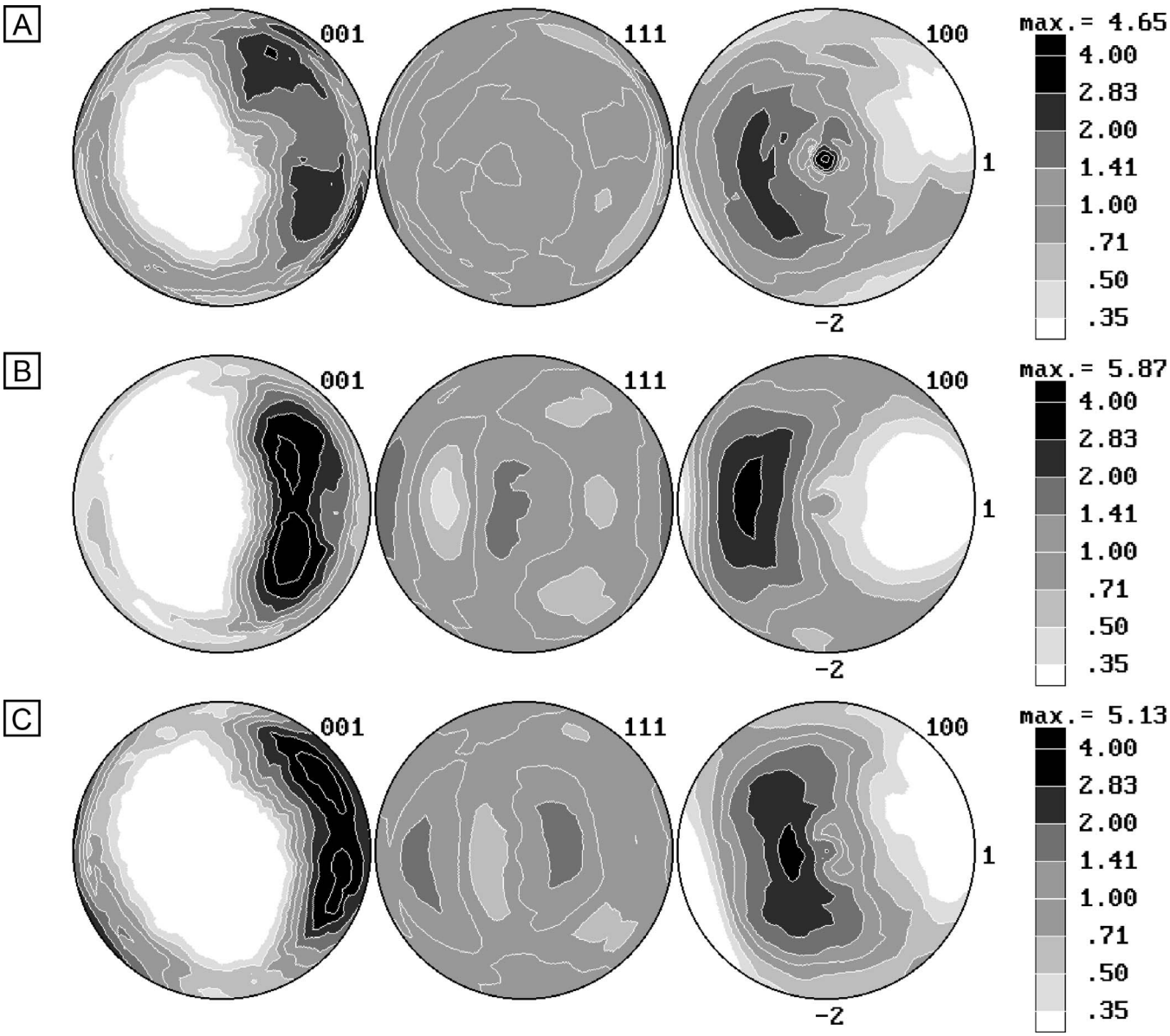

FIGURE 4—Surface textures shown through (001), (111), and (100) pole figures. Values are in multiples of random orientations (m.r.m.) (random = 1.00) and white areas show orientations with less than 35% of that expected for random distribution. Maximum values are close to 5 m.r.m. A) Modern shell. B) Holocene shell. C) Pleistocene shell.

Other divalent elements (Mg, Fe^{2+}, Mn^{2+}) have smaller ionic radii (Fe^{2+} 0.92 Å, Mn^{2+} 0.96 Å, Mg^{2+} 0.89 Å in eightfold coordination), so their substitutions are much more limited. Iron and Mn are usually below their detection limits, whereas Mg was detected in about half of the analyses but in very minor amounts (up to 0.04 wt% MgO).

Lead, Ba, and K were found to be below their detection limits. Pilkey and Goodell (1964) detected changes in Ba content among modern and fossil bivalves, but they report a concentration for this element up to a few tens of ppm (and hence undetectable by electron microprobe).

Among the anions, sulfur reaches 0.19 wt% (as SO_3), whereas P can be as high as 0.21 wt% (as P_2O_5). Chlorine ranges up to 0.12 wt% Cl. Concentration gradients were observed for Na, Sr, Cl, S, and P in the modern valve (Fig. 7), but with the exception of Sr, concentrations tend to be more uniform across the shells of older specimens. It is noteworthy that flattening of profiles occurs early in the diagenetic history, as the trace-element contents of Holocene and Pleistocene valves are much more alike.

In the modern shell, three zones can be differentiated on a chemical basis, each of them with fine-scale oscillations (Fig. 7). The inner zone is separated from the intermediate zone by a sharp discontinuity (except for Cl, which remains approximately constant across this contact), where Sr and S drop, and Na starts to rise. The intermediate zone is characterized by low contents of Cl, Sr, and S, and a steady increase of Na. Sodium falls abruptly at the contact with the outer zone, repeating the pattern of the previous zone. Chlorine and sulfur also increase markedly in the outer zone, whereas strontium concentration remains low. These three zones can be correlated with structural changes. The inner zone coincides with the microstructural layer where bands are parallel to the interior of the shell. The intermediate zone coincides with the layer where bands are at an angle to the interior, whereas the outer zone coincides with the microstructural layer where bands are almost at a right angle to the surface. This zoning can be seen in the element-distribution map showing variations of Sr in a sector of the modern and Pleistocene shells, where the decrease in Sr concentration coincides with the layer boundary. No variation is evident in the Pleistocene shell (Fig. 8).

A comparison of the chemical composition of valves of different ages shows trends of decreasing Na, Sr, and (to a lesser degree) Mg with increasing age. Sulfur and P are strongly depleted in the Holocene and Pleistocene shells, and their gradients are virtually erased.

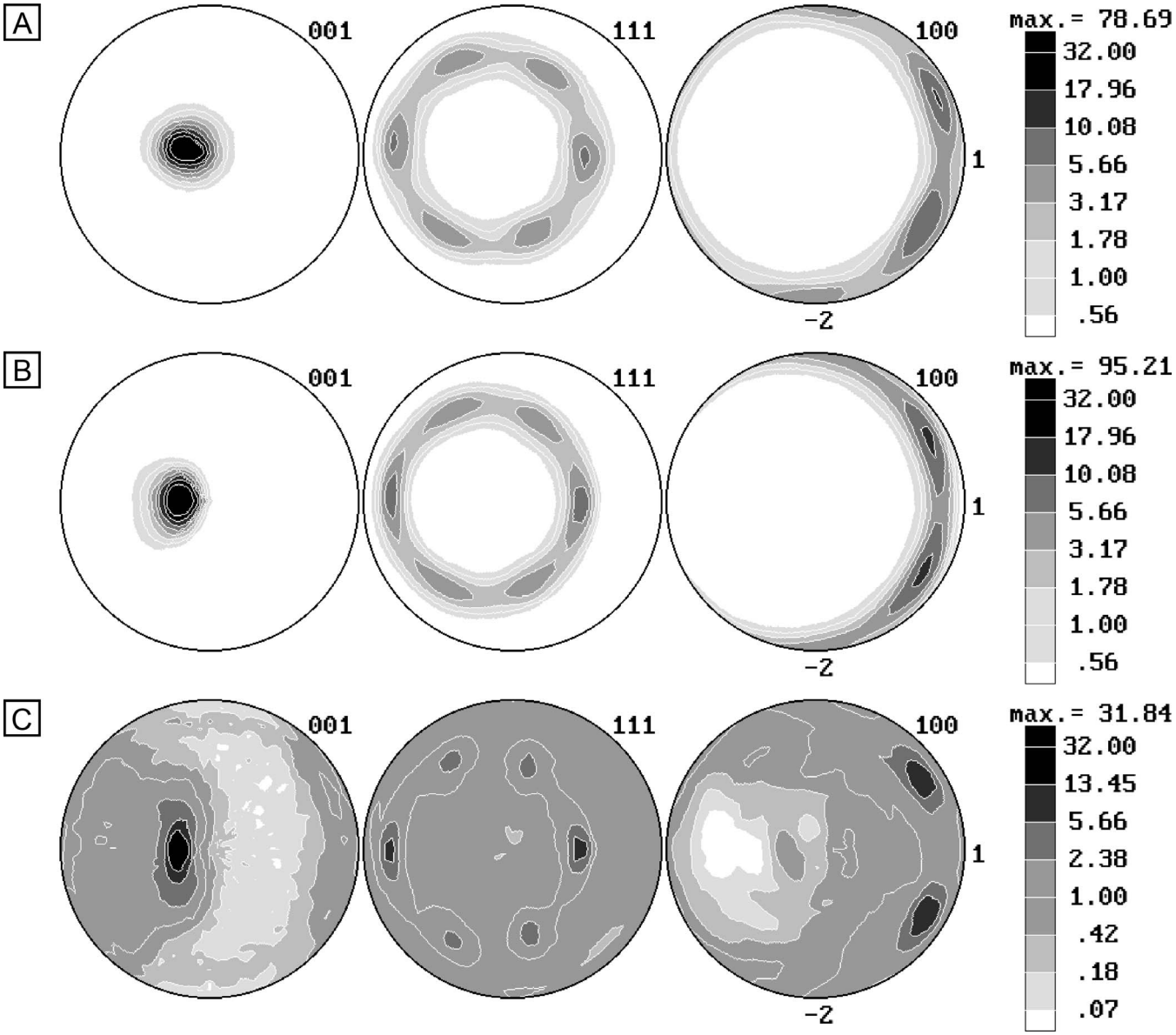

FIGURE 5—Texture on the inner layer of the Holocene specimen showing twinning with pseudohexagonal symmetry. Values are in multiples of random orientations (m.r.m.) (random = 1.00), and white areas show orientations with less than 56% of that expected for random distribution. Maxima are much higher than on the surface, with values of at least 32 m.r.m for the Pleistocene shell, showing a high decrement with respect to younger ones. A) Modern shell. B) Holocene shell. C) Pleistocene shell.

Microindentation

Figure 9 shows the Vickers microhardness of modern, Holocene, and Pleistocene samples. The microhardness values are larger for the Pleistocene and Holocene valves than for the modern valves. The area of chipped regions for the highest load is displayed in Figure 10. Results are less conclusive for the smaller loads, where the chipped areas are difficult to discern from the indentation itself. The modern specimens show the least hardness together with the fewest chipped regions, which is consistent with their ability to withstand higher elastic deformations without fragmenting due to the presence of the organic matrix. A test spot where chipping occurred is shown in Figure 11.

DISCUSSION

Diagenetic Changes

Textural Modifications.—Mineralogy remains constant, with aragonite as the only crystalline phase throughout the entire examined time interval, but texture (as revealed by XRD, SEM, and optical microscopy; Figs. 1, 3) is modified. The Pleistocene valve shows more grains in a random distribution, compared with the twinning pattern evident in modern and Holocene shells (Figs. 3–4). The approximate constant value of crystallite size suggests that the dissolved $CaCO_3$ does not precipitate in crystallographic continuity with the preexisting crystals, as this would lead to larger crystallite size (hence narrower diffraction peaks) and a sharpening of the twinning pattern. A possible explanation which remains to be tested is that aragonite cement occupies voids left by degraded organic matrix, as found by Webb et al. (2007).

Dissolution and reprecipitation is also indicated by the gradual blurring of the banding pattern with increasing age (see Pilkey and Goodel, 1964). Similar observations were reported for coral skeletons at a very early stage of diagenesis, with a marked decrease of banding pattern (Perrin and Cuif, 2001; Perrin, 2004).

Pingitore (1976) found differences in host-cement relationships produced during the polymorphic transformation of aragonite to calcite in vadose and phreatic environments. Transformation in a

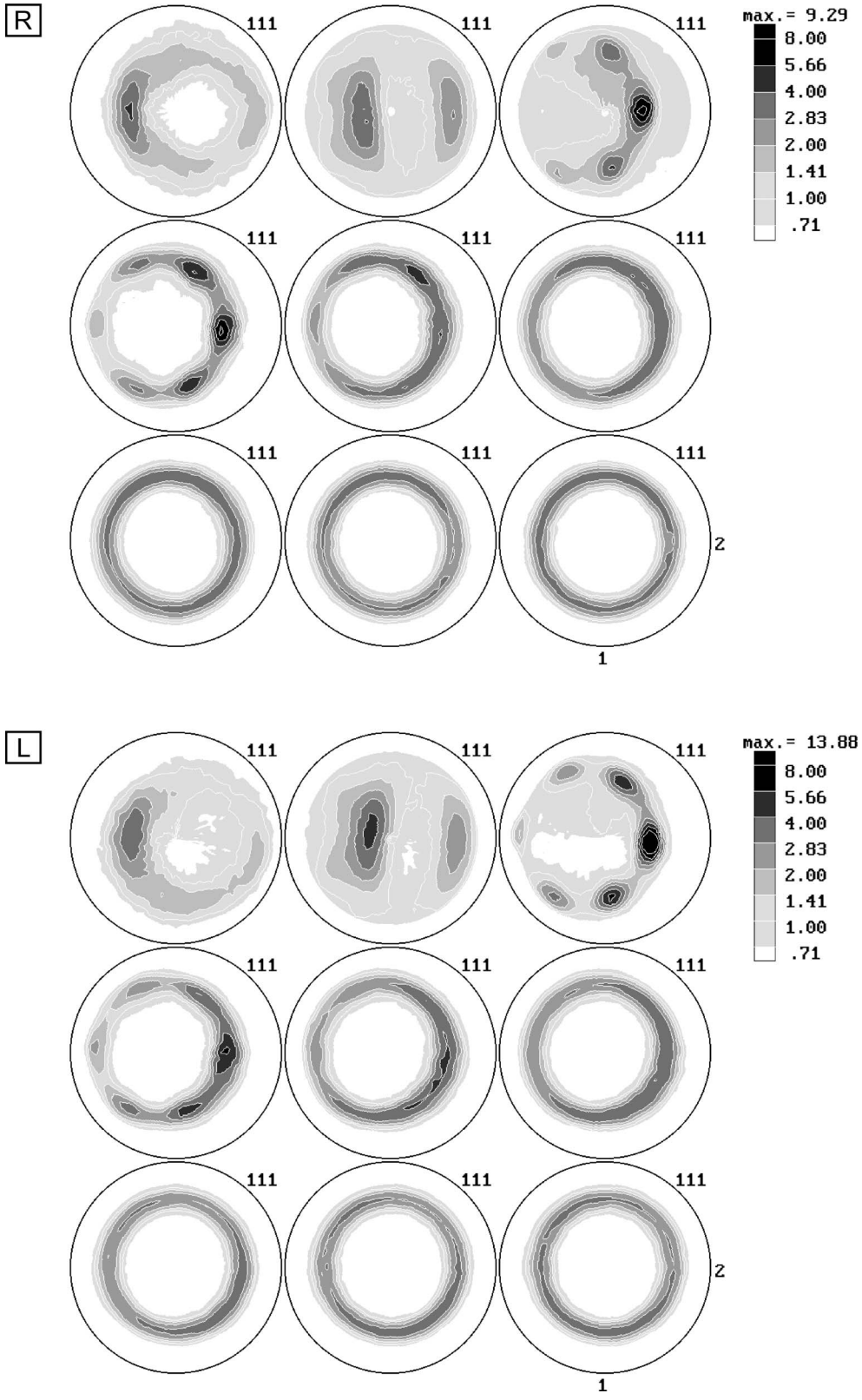

FIGURE 6—Texture at the same depths between the right and left shells from the same modern specimen showing variations in textures in the same organism. R) Right shell. L) Left shell.

vadose zone proceeds along thin-film solution fronts, producing neomorphic calcite of smaller (<100 μm) crystal size abutting on former skeletal walls.

This contrasts with calcite precipitated in phreatic zones, which forms mosaics of larger crystals (sometimes reaching a few mm long), crosscutting former skeletal structures (Pingitore, 1976). Fine structural details tend to be preserved in vadose environments, whereas they are obliterated in phreatic environments. According to Sandberg and Hudson (1983), when the process occurs in a shallow-marine environment it shares the textural characteristics of diagenesis in the phreatic zone.

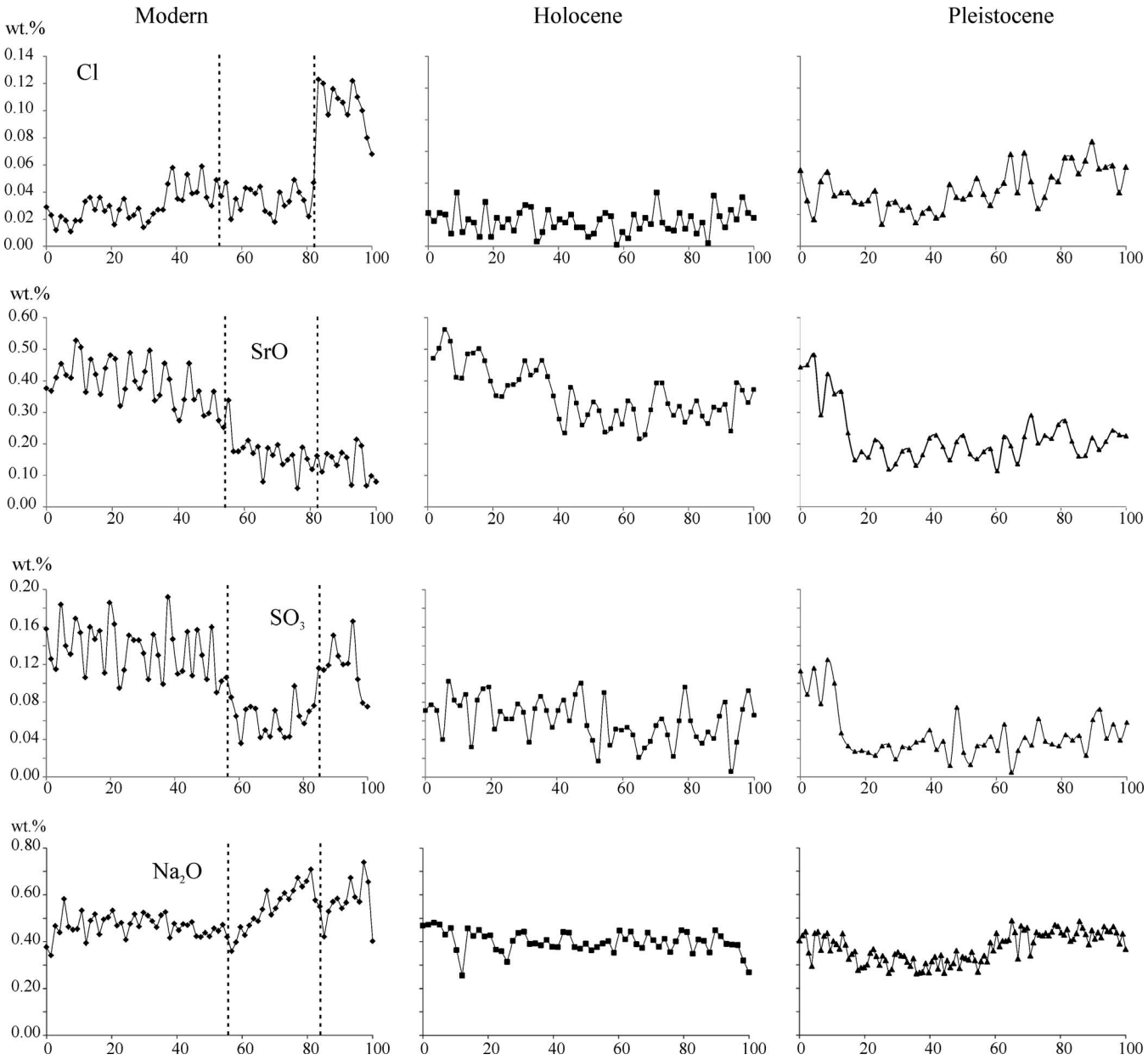

FIGURE 7—Compositional profiles measured with electron microprobe across *A. purpurata* shells. Along the abscissa, 0 marks the point closest to the inner surface, and 100 is the point closest to the outer surface. The same vertical scale applies to each row. Vertical dashed lines in the diagrams of the modern shell mark the transition from one microstructural zone to another (see text for details).

The microstructures shown by fossil shells of *A. purpurata* are similar to those produced in a vadose zone.

Changes in Chemical Composition.—Both abiotic and biotic factors influence the trace-element content in $CaCO_3$ polymorphs. Examples of abiotic factors are the abundance and ratios of elements in seawater, temperature, precipitation rate, and elemental selectivity of a given crystal face conditioned by its atomic structure; body fluid chemistry, organic matrix concentration and composition, and physiological influences are among the biotic factors (Grossman et al., 1996).

Compositional gradients, if existent, are blurred with increasing age, thus indicating diffusion or a dissolution and reprecipitation process. Some elements that display fairly homogeneous concentrations are also depleted in older shells (Fig. 7).

Trends of decreasing Na, S, and Sr with increasing diagenesis, interpreted as the result of loss during neomorphic inversion of aragonite to calcite, have been documented by a number of authors (e.g., Veizer, 1983; Popp et al., 1986; Al-Aasm and Veizer, 1986; Grossman et al., 1996; Oliver et al., 1996). In contrast, aragonite is the only detectable phase in *A. purpurata* shells, so the observed chemical changes cannot be related to variations in partition coefficients of minor and trace elements for different $CaCO_3$ polymorphs.

We favor the hypothesis that chemical variations are due to dissolution and reprecipitation of aragonite through a thin film of solutions of meteoric origin in small-scale, semiclosed microenvironments. At the same time, this led to the retention of microstructures (cf., Pingitore, 1976; Brand and Veizer, 1980; Al-Aasm and Veizer, 1986). The higher Na loss compared to that of Sr is probably related to the fact that Sr is more readily accommodated by the aragonite structure, and also because diagenetic meteoric waters have a lower Na/Ca than Sr/Ca ratio (Al-Aasm and Veizer, 1986). Since Na may also be accommodated by the organic matrix, the degradation of such may contribute to the lowered concentrations.

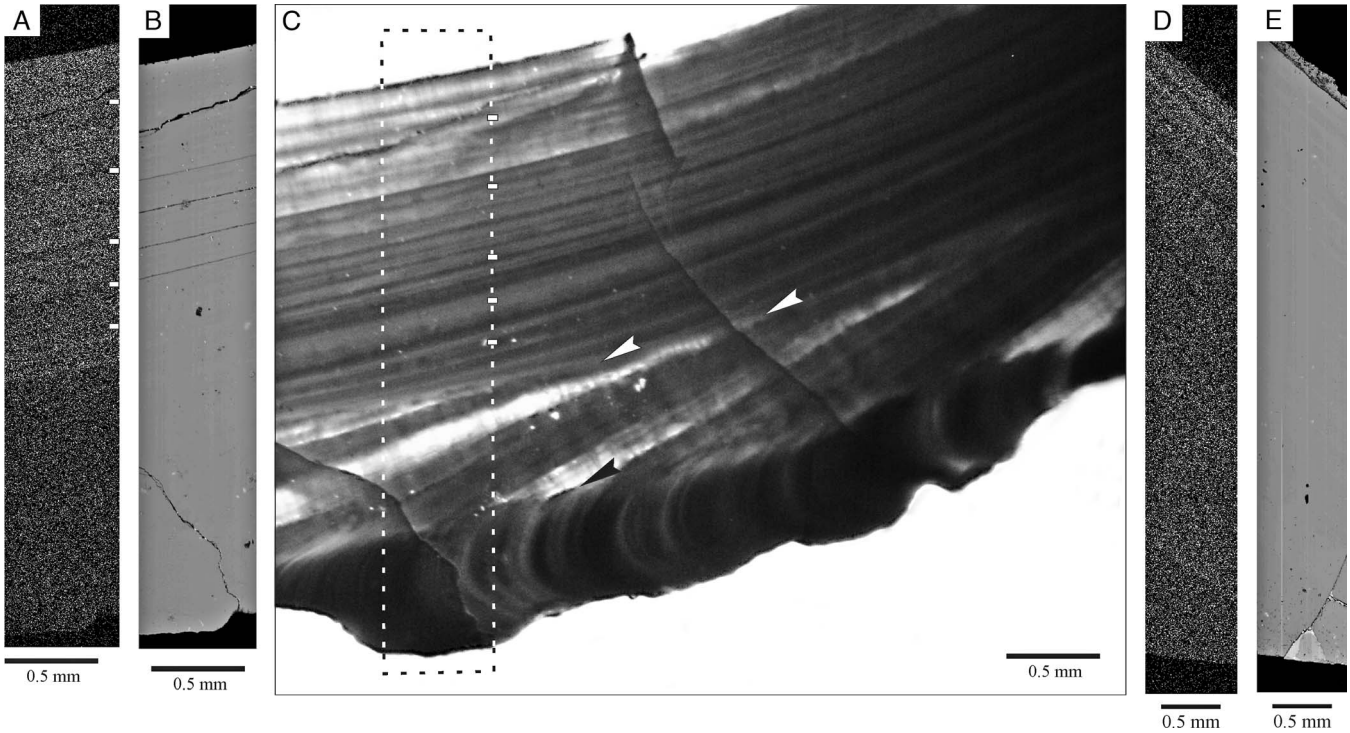

FIGURE 8—A) Elemental map showing the distribution of Sr in a modern shell. There is a sharp boundary between Sr-rich and Sr-poor regions. The low contrast of the map is due to the reduced concentration of Sr in the shell. Horizontal bars at the right margin mark some bands relatively depleted in Sr. B) Backscattered electron image of the same zone, showing the overall compositional homogeneity. The thin lines in the upper part of the image are fissures extending along layer contacts, and do not represent compositional changes. C) Photomicrography of the shell (plane polarized light, parallel polars); the dashed box marks the area shown in images A and B. Note that the bands with lower Sr content (marked by horizontal bars, as in A) do not correspond to color changes. Arrows mark the boundary between the inner and intermediate (light) and intermediate outer (black) layers. D) Elemental map showing the distribution of Sr in a Pleistocene shell. Only a thin margin is enriched in Sr (also seen in quantitative analyses, Fig. 7). Otherwise, the Sr content is low and relatively homogeneous. E) Backscattered electron image of the same zone, showing the overall compositional homogeneity.

Strontium displays an interesting behavior. In addition to an overall decrease of Sr outward, Sr shows cyclical variations in the direction of shell growth, which possibly result from metabolic activity related to temperature, salinity, and growth rate during the life of the individual. Similar features have been found in brachiopods (Lowenstam, 1961), in *Mytilus* sp. (Dodd, 1966), and in aragonite bivalves (Purton et al., 1999; Gillikin et al., 2005). Other studies have reported that Sr is heterogeneously distributed laterally across the growth bands of the bivalve *Artica islandica*, probably controlled by a complex interaction of temperature with biological and kinetic processes (Foster et al., 2009; Zhang, 2009; Schöne et al., 2010). The compositional gradient disappears in the Holocene valve, but Sr seems to be redistributed within the same shell, as shown by more even but still high Sr contents. The Pleistocene valve has much lower Sr concentration. Since Sr diffusion rates in carbonates are extremely slow (Finch and Allison, 2003), the increased homogeneity in older valves suggests a fluid-assisted redistribution and leaching of Sr. This coincides with the findings of several authors (e.g., Stehli and Hower, 1961; Bruckschen et al., 1995) who mention that Sr (along with Mg, Mn, and Ba) is usually leached, although the opposite behavior has also been documented (Krinsley, 1960).

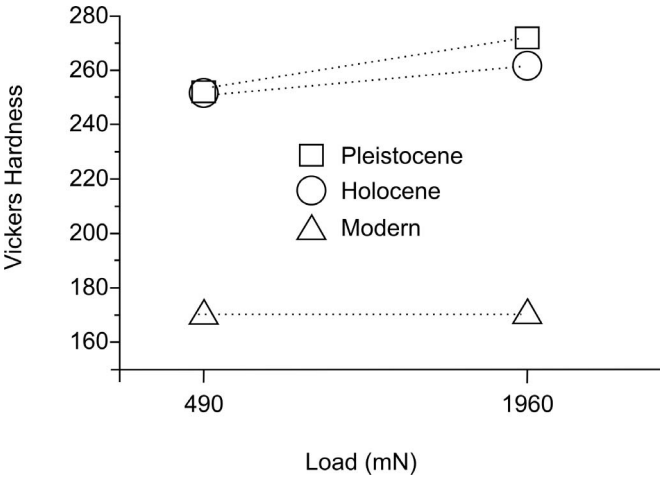

FIGURE 9—Microhardness of modern, Holocene, and Pleistocene samples.

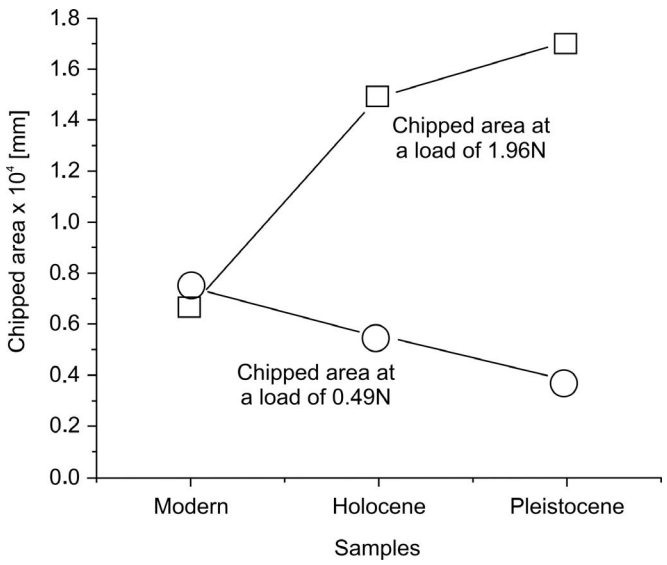

FIGURE 10—Chipped areas at a load of 0.49 N and 1.96 N in relation to the age.

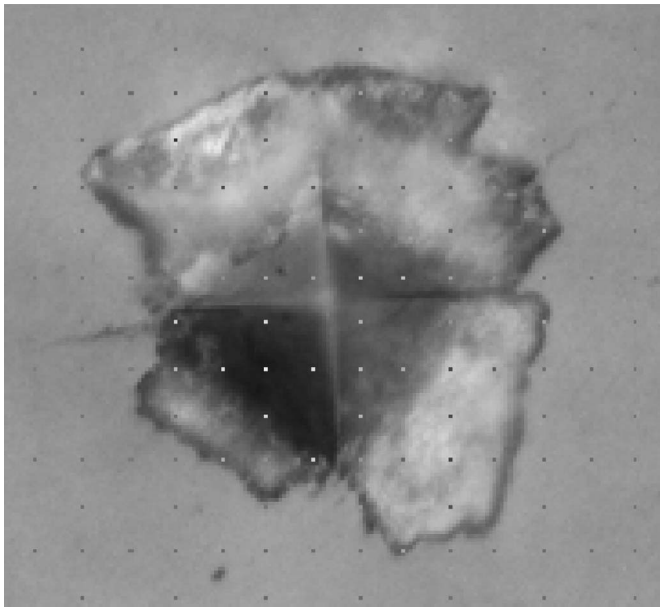

FIGURE 11—Photograph of an indentation presenting chipping. Because of the high hardness of the shell, the energy is dissipated by surface scaling.

Phosphorus and especially sulfur are depleted in older valves. Given the marked size, coordination geometry, and charge (for P^{5+}) differences between these elements and $(CO_3)^{2-}$ groups, it is very likely that their diminished concentrations are at least partially related to degradation of organic matter, although sulfur (as SO_4^{2-}) has been shown to substitute for $(CO_3)^{2-}$ groups to a small degree in the calcite structure (Busenberg and Plummer, 1985; Pingitore et al., 1995). Part of the sodium may also be bound in organic compounds. A comparison of the evolution of microstructural and chemical changes shows that the microstructural adjustments are more sluggish than chemical modifications produced by diagenetic processes.

Changes in Mechanical Resistance.—In terms of mechanical properties, the resistance to fracture of shells is characterized by the measurement of their strength (Rhoads and Lutz, 1980; Zuschin and Stanton, 2001; Allison and Bottjer, 2011; Yang et al., 2011a, 2011b). A study performed on scleractinian corals showed that diagenesis in those organisms was very early and rapid, with appreciable changes just a few years after the coral's death (Perrin and Smith, 2007). Other studies have documented the inverse relationship between age and the amount of soluble intraskeletal compounds that can be extracted from fossils (van der Meide et al., 1980; Collins et al., 1991; Gautret and Marin, 1993; Gautret and Aubert, 1993; Gautret, 2001).

The degradation of the organic polymeric binder results in greater hardness, a loss of integrity, and easier cracking. Despite the fact that the cracking tendency is one of the mechanisms used by the shell to resist catastrophic breaking, the reduction in the amount of organic binder makes the material much more fragile and renders it less adequate for protection. Furthermore, there is a need for self-repair time that is possible only under low-damage circumstances. In this study, degradation of the organic matrix means enough loss of the original polymeric structure of the organic matter so as to lead to a diminished functionality; that loss could be partial or total.

The mechanical properties of the valves, such as the ability to transfer charges between adjacent layers of aragonite (Liang et al., 2008), are associated with the structure and functions of the biological matrix which also promotes the formation of the crystalline layers (Rhoads and Lutz, 1980). The studied shells from the Holocene and the Pleistocene show higher Vickers hardness and a more fragmented area than the modern shells (Figs. 9–10). This indicates that over time, less than 5000 years, the valves of *A. purpurata* have become harder but more brittle.

The evidence discussed above suggests that this change in mechanical resistance to physical stress is mainly determined by recrystallization leading to the obliteration of the crossed-lamellar structure, together with the degradation of organic matrix, which confers distinctive bending capabilities and toughness to the material (Purdy, 1968; Zuschin and Stanton, 2001; Tong et al., 2002; Neves and Mano, 2005) and protects it from crystallite-by-crystallite disintegration (Zuschin and Stanton, 2001). The fact that hardness increases sharply in the Holocene sample, but microstructural changes (as evidenced by X-ray diffraction) are incipient, suggests that the degradation of organic matter plays a key role in the hardness and chipping behavior in *A. purpurata* shells. The most important changes are clearly evident in valves younger than 5000 years, implying that degradation of organic matter occurs early in the diagenetic process; the slight hardness and fragility increase in the Pleistocene shell could also be caused by advanced aragonite recrystallization, along with a more pronounced degradation of the remaining organic matrix.

The shell microstructure causes anisotropic behavior when exposed to microhardness tests. Damage is greater when the test point is directed perpendicular to the outer shell surface (i.e., at high angles to the second-order lamellae), decreasing when the load is applied parallel to growth lines (Yang et al., 2011b). In a natural environment, during diagenesis, most of the shells are compressed perpendicularly to their outer surfaces, as this is the most stable position in which shells are deposited. Pressure is therefore applied along the direction of greatest potential damage.

Additional Implications

In this contribution we have shown that *A. purpurata* valves have undergone subtle crystallographic and chemical changes related to the very early diagenetic processes. This has some additional consequences that we will explore below.

Inferring Environmental Conditions Based on Shell Preservation.—*Amiantis purpurata* has been the dominant species in the benthic community of Bahía San Antonio from the Pleistocene up to the present day (Morsán, 2000, 2003; Navarte et al., 2007; and M.S. Bayer, S. Gordillo, and E. Morsan, own unpublished data, 2013). Benevolent biostratinomic characteristics of the area, as evidenced by the signs of good preservation of the analyzed specimens, allowed the fossilization of a large amount of *A. purpurata* shells, thus reflecting their true abundance in Bahía San Antonio.

Furthermore, in rich shell deposits and modern beach assemblages, the time span between the oldest and the youngest shell can be from hundreds to several thousand years, presenting different degrees of material preservation (Kidwell and Bosence, 1991; Kidwell and Flessa, 1995; Olszewski, 2004). This has been called sedimentological time-averaging (Kowalewski, 1996; Kidwell, 1998; Fujiwara et al., 2004). This phenomenon occurs on the beaches of Bahía San Antonio, where large assemblages of *A. purpurata* shells with temporal mixing show varying degrees of preservation. The oldest shells are represented in smaller amounts compared to modern valves in the same deposit, because the oldest ones are more fragile and therefore more susceptible to physical stress (biostratinomic) than younger ones (Olszewski, 1999).

Kowalewski et al. (1995) proposed using the degree of fragmentation (plotted in a ternary diagram with the apexes poor, regular, or good) in order to compare the preservation state of shells. As mentioned above, the shells of *A. purpurata* become more fragile with increasing age. Though this should cause no major problems in undisturbed deposits, if the sediments are reworked these valves would fracture much more easily than their younger equivalents. This may lead to the incorrect conclusion of an environment being more energetic than it really is.

Using Sr Content for Paleoenvironmental Studies.—The Sr/Ca and Mg/Ca ratios in carbonate exoskeletons have been used to quantify water temperature during biomineralization. However, this approach

has been objected to by other researchers, who found departures of thermodynamic equilibrium and contradictory behavior, even among specimens sampled from the same site (see Schöne et al., 2010 and references therein). Schöne et al. (2010) detected markedly different concentrations of Sr, and especially Mg, in the organic matrix and the carbonates, and attributed the erratic variations to the analysis of mixtures, in varying proportions, of calcium carbonates and organic compounds.

The fact that Sr can reach a few thousand ppm in *A. purpurata* shells (thus being easily measurable by a variety of methods, including electron microprobe) makes this bivalve an interesting target for calibration of the relationship between temperature and composition. In addition to studies designed to evaluate the impact of insoluble organic matrix on the Sr/Ca ratio, three additional facts should be taken into account. First, there are oscillations, probably due to metabolic activity related to water temperature, salinity, and growth rate (Purton et al., 1999); for this reason, methods that analyze a very small spot (like EPMA) should be used, otherwise, an average will be obtained. Second, modern shells show variations in Sr content depending on the structural zone being considered; and third (even if only one zone was compared among different samples), Sr is redistributed early during diagenesis. For these reasons, *A. purpurata* is a rather poor candidate for paleoenvironmental studies based on the Sr content, even after accounting for the influence of organic matrix. While a study on the impact of these cryptic diagenetic changes on the Sr isotopic composition of *A. purpurata* is outside the scope of this contribution, appreciable changes in Sr concentration indicate that the system was at least partially open. It is unknown if this redistribution and removal of Sr is associated with an isotopic fractionation, but until this issue is resolved, great caution must be used when applying isotopic techniques to paleoenvironmental studies.

Mineralogical Changes as Evidence of Diagenetic Alteration.—A number of studies have shown that in aragonitic shells, the main diagenetic mineralogical change in a meteoric environment is the dissolution of aragonite and/or precipitation of calcite cement (e.g., Folk, 1974; Allan and Matthews, 1982; Morse et al., 1997; Magnani et al., 2007). Therefore, a first screening is usually carried out using X-ray diffraction to discard those specimens that show anomalous mineralogy, such as the presence of calcite in valves that are assumed to be composed entirely of aragonite (Zhou et al., 1999). Shells that do not show signs of anomalous compositions may then be used with greater confidence for further research, such as isotopic or trace-element studies.

Aragonite is the only detectable phase in XRD of *A. purpurata* measured at a speed of 0.7 s step^{-1} [approximately 2° (2θ) per minute]. However, a very weak hump is visible around 29.5° (2θ), where the most intense reflection of calcite is to be expected. In order to test this, scans were made between 27.5° and 30.5° (2θ) with a counting time of 10 s per step. The peak is now very clearly seen, confirming the presence of calcite. The intensity of the peak is the same in modern, Holocene, and Pleistocene samples, i.e., it does not vary with age.

This leads to three different possibilities: (1) calcite is a diagenetic mineral; (2) calcite is indeed present in *A. purpurata* valves and has been previously overlooked; or (3) it formed during the sample preparation steps. Hypothesis 1 was rejected because calcite is evident in a modern specimen, which had died at the most a few days before being collected, as evidenced by soft tissue still present. Hypothesis 2 was rejected because no calcite was detected in XRD measured in valves that had been ground flat but not powdered. To test hypothesis 3, a crystal of inorganic aragonite from Morocco was prepared for XRD following the same procedure used for the shells. The peak at ~29.5° (2θ) was also clearly detected, with approximately the same intensity as in the bivalve shells. We therefore conclude that aragonite undergoes a polymorphic transformation to calcite even under the mild conditions used for sample preparation (see the Methods section for details).

The conclusion drawn from these experiments is that a very small amount (in our case about 0.4 wt%) of calcite in *A. purpurata* shells should not necessarily be taken as indicative of diagenesis, and the samples can still be used for studies that require as little postmortem modification as possible. Of course, we do not contend that the valves that do not show calcite (or when calcite can be assumed to be an artifact of sample preparation) always behaved as an isotopically closed system; each case should be further evaluated on its own merits.

CONCLUSIONS

In our study, age is a critical factor with respect to the resistance to breakage, since it determines what would be preserved in the fossil record. Observable differences between modern and fossil specimens are noticed as a consequence of early diagenesis. (1) The original aragonitic structure of the shells remained during aging, and did not transform to calcite during a period of time that exceeds 100,000 years. (2) General structure is well preserved, while microstructures display increasing textural changes with time. (3) The regularity of the crystallographic texture decreases through the ages. (4) The microstructures show by fossil shells of *A. purpurata* are coincident with a vadose zone. (5) Changes in element profiles occur early on in diagenesis, before the shells reach an age of 5000 years. (6) Chemical variations are due to recrystallization of aragonite by dissolution and reprecipitation through a thin-film solution of meteoric origin in small-scale, semiclosed microenvironments. (7) The hardness of the shells, as well as their fragility, increases with age of deposit, which could be a consequence of the degradation of skeletal organic matrix. (8) The alteration of the organic matrix in the studied shells occurred before the shells reach the age of 5000 years.

ACKNOWLEDGMENTS

Diego Balseiro and Diego F. Muñoz provided valuable comments and suggestions during the preparation of this manuscript. Fernando Gómez is kindly acknowledged for a critical reading of the manuscript. All of the above belong to CICTERRA, CONICET-UNC. Raúl Carbonio (INFICQ) is thanked for granting access to the diffractometer. Dr. C. Perrin and an anonymous reviewer made valuable suggestions that considerably improved the manuscript.

REFERENCES

Addicott, W.O., 1973, Oligocene molluscan biostratigraphy and paleontology of the Lower Part of the type Temblor Formation, California: United States Geological Survey Professional Paper, v. 791, p. 1–48.

Al-Aasm, I., and Veizer, J., 1986, Diagenetic stabilization of aragonite and low-Mg calcite, I. Trace elements in rudists: Journal of Sedimentary Petrology, v. 56, p. 138–152.

Allan, R.J., and Matthews, G.K., 1982, Isotope signatures associated with early meteoric diagenesis: Sedimentology, v. 29, p. 797–817.

Allison, P.A., and Bottjer, D.J., 2011, Taphonomy, Second Edition, Process and Bias through Time, vol. 32, *in* Landman, N.H., and Harries, P.J., series eds., Topics in Geobiology: Springer, Dordrecht, 599 p.

Angulo, R., Fidalgo, F., Gomez Peral, M., and Schnack, E., 1978, Las ingresiones marinas Cuaternarias en la Bahía de San Antonio y sus vecindades, Prov. De Rio Negro: VII Congreso Geológico Argentino, p. 271–283.

Bayer, M.S., Gordillo, S., and Fucks, E., 2010, Análisis tafonómico en *Amiantis purpurata* (L.) (Bivalvia): Una clave para descifrar el paleoambiente del Cuaternario en el Golfo San Matías (Río Negro, Argentina): Décimo Congreso Argentino de Paleontología y Bioestratigrafía. La Plata, p. 111.

Bolmaro, R.E., 2005, *Amiantis purpurata* and *Eurhomalea lenticularis*: Two case studies of oriented mineralization and its influence on clam shells strength, *in* Arias, J.L., and Fernández, M.S., eds., Proceedings of the 9th International Symposium on Biomineralization, Pucón, Chile: Editorial Universitaria, Santiago, Chile, p. 237–246.

Boretto, G.M., Gordillo, S., Colombo, F., Cioccale, M., and Fucks, E., 2013, Multi-proxy evidence of late Quaternary environmental changes in the coastal area

of Puerto Lobos (Northern Patagonia, Argentina): Quaternary International, http://dx.doi.org/10.1016/j.quaint.2013.02.017.

Borodin, V.L., Lyutin, V.I., Ilyukhin, V.V., and Belov, N.V., 1979, The isomorphous series calcite-otavite: Doklady Akademii Nauk SSSR, v. 245, p. 1099–1101.

Brand, U., 1989, Aragonite-calcite transformation based on Pennsylvanian molluscs: Geological Society of America Bulletin, v. 101, p. 377–390.

Brand, U., and Veizer, J., 1980, Chemical diagenesis of a multicomponent carbonate system; 1, Trace elements: Journal of Sedimentary Research, v. 50, p. 1219–1236.

Bruckschen, P., Bruhn, F., Meijer, J., Stephan, A., and Veizer, J., 1995, Diagenetic alteration of calcitic fossil shells: Proton microprobe (PIXE) as a trace element tool: Nuclear Instruments and Methods in Physics Research B, v. 104, p. 427–431.

Busenberg, E., and Plummer, L.N., 1985, Kinetic and thermodynamic factors controlling the distribution of SO_4^{2-} and Na^+ in calcites and selected aragonites: Geochimica et Cosmochimica Acta, v. 55, p. 777–785.

Chateigner, D., Hedegaard, C., and Wenk, H.R., 2000, Mollusc shell microstructures and crystallographic textures: Journal of Structural Geology, v. 22, p. 1723–1735.

Chateigner, D., Ouhenia, S., Krauss, C., Belkhir, M., and Morales, M., 2010, Structural distortion of biogenic aragonite in strongly textured mollusk shell layers: Nuclear Instruments and Methods in Physics Research B, v. 268, p. 341–345.

Chave, K.E., 1964, Skeletal durability and preservation, *in* Imbrie, J., and Newell, N., eds., Approaches to Paleoecology: John Wiley and Sons, New York, p. 377–387.

Cherns, L., and Wright, V.P., 2009, Quantifying the impacts of early diagenetic aragonite dissolution on the fossil record: PALAIOS, v. 24, p. 756–771.

Cherns, L., Wheeley, J.R., and Wright, V.P., 2011, Taphonomic bias in shelly faunas through time: Early aragonitic dissolution and its implications for the fossil record: Taphonomy Topics in Geobiology, v. 32, p. 79–105.

Collins, M.J., Muyzer, G., Curry, G.B., Sandberg, P., and Westbroek, P., 1991, Macromolecules in brachiopod shells: Characterization and diagenesis: Lethaia, v. 24, p. 387–397.

Cutler, A.H., 1995, Taphonomic implications of shell surface textures in Bahía la Choya, northerm Gulf of California: Palaeogeography, Palaeoclimatology, Palaeoecology, v. 114, p. 219–240.

Dalbeck, P., England, J., Cusack, M., Lee, M.R., and Fallick, A.E., 2006, Crystallography and chemistry of the calcium carbonate polymorph switch in *Mytilus edulis* shells: European Journal of Mineralogy, v. 18, p. 601–609.

Da Silva Forti, I.R., 1969, Cenozoic mollusks from the drillholes Cassino and Palmares do Sul of the Coastal Plain of Rio Grande do Sul: Iheringia Geologia, v. 2, p. 55–155.

Del Rio, C.J., 2000, Malacofauna de las Formaciones Paraná y Puerto Madryn (Mioceno marino, Argentina): Su origen, composición y significado bioestratigráfico: INSUGEO, Serie Correlación Geológica, v. 14, p. 77–101.

De Renzi, M., and Ros, S., 2002, How do factors affecting preservation influence our perception of rates of evolution and extinction? The case of bivalve diversity during the Phanerozoic, *in* De Renzi, M., Pardo, M.V., and Belinchón, M, eds., Current Topics on Taphonomy and Fossilization: Collecció Encontres, Valencia, Spain, p. 77–88.

Dettman, D.L., and Lohmann, K.C., 2000, Oxygen isotope evidence for high-altitude snow in the Laramide Rocky Mountains of North America during the Late Cretaceous and Paleogene: Geology, v. 28, p. 243–246.

Do Campo, M.D., 1991, Composición mineralógica de conchillas de moluscos marinos actuales de la Costa Atlántica Argentina: Revista de la Asociación Geológica Argentina, v. 46, p. 87–92.

Dodd, J.R., 1966, Diagenetic Stability of Temperature-Sensitive Skeletal Properties in *Mytilus* from the Pleistocene of California: Geological Society of America Bulletin, v. 77, p. 1213–1224.

Duarte, G.A., De Vincentis, N.S., Charca Ramos, G., and Bolmaro, R.E., 2008, Mechanical properties of hard tissue malacological materials. Measuring failure energy by microindentation and milling: 18 Congresso CBECIMAT, Porto de Galinhas, Brasil, p. 93.

Fan, M., and Dettman, D.L., 2010, Late Paleocene high Laramide ranges in northeast Wyoming: Oxygen isotope study of ancient river water: Earth Planetary Science Letters, v. 286, p. 110–121.

Favier Dubois, C.M., 2009, Valores de efecto reservorio marino para los últimos 5000 años obtenidos en concheros de la costa atlántica nordpatagónica (Golfo San Matías, Argentina): Magallania, v. 37, p. 139–147.

Feige, A., and Fürsich, F.T., 1991, Taphonomy of the Recent molluscs of Bahía la Choya (Gulf of California, Sonora, Mexico). *In* Fürsich, F.T., and Flessa, K.W., eds., Ecology, taphonomy, and paleoecology of Recent and Pleistocene molluscan fauna of Bahia la Choya, northern Gulf of California: Zitteliana, München, p. 89–134.

Fernández López, S.R., 2000, Tafonomía: Departamento de Paleontología, Universidad Complutense de Madrid, Madrid, 167 p.

Feruglio, E., 1950, Descripción geológica de la Patagonia: Dirección General de Yacimientos Petrolíferos Fiscales, 437 p.

Fidalgo, F., and Ricci, J.C., 1970, Consideraciones geomórficas y sedimentológicas sobre los Rodados Patagónicos: Revista de la Asociación Geológica Argentina, v. 25, p. 430–443.

Finch, A.A., and Allison, N., 2003, Strontium in coral aragonite: 2. Sr coordination and the long-term stability of coral environmental records: Geochimica et Cosmochimica Acta, v. 67, p. 4519–4527.

Folk, R.L., 1974, The natural history of crystalline calcium carbonate: Effects of magnesium content and salinity: Journal of Sedimentary Petrology, v. 44, p. 40–53.

Forbes, E., 1856, Tertiary fluvio-marine formation of the Isle of Wight: Memoirs of the Geological survey of Great Britain and of the Museum of Practical Geology, p. 1–162.

Foster, L.C., Allison, N., Finch, A.A., and Anderson, C., 2009, Strontium distribution in the shell of the aragonite bivalve *Arctica islandica*: Geochemistry, Geophysics, Geosystems, v. 10, p. 3.

Frassinetti, D.C., and Covacevich, V.C., 1993, Bivalvos del Mioceno marino de Matanzas (Formación Navidad, Chile Central): Boletín del Museo de Historia Natural de Santiago de Chile, v. 44, p. 73–97.

Fucks, E.E., Schnack, E.J., and Charó, M., 2012, Aspectos geológicos y geomorfológicos del sector N del Golfo San Matías, Río Negro, Argentina: Revista de la Sociedad Geológica de España, v. 25, p. 95–105.

Fujiwara, O., Kamataki, T., and Masuda, F., 2004, Sedimentological time-averaging and 14C dating of marine shells: Nuclear Instruments and Methods in Physics Research B, v. 223–224, p. 540–544.

Gautret, P., 2001, Biochemical features of intraskeletal organic matrices within sponge and coral aragonite: Implications for diagenetic pathways: Bulletin of the Tohoku University Museum, v. 1, p. 155–163.

Gautret, P., and Aubert, F., 1993, Comparaison des matrices organiques solubles intrasquelettiques d'Acropora (Scléractiniaire) des récifs actuels et du Pléistocène de Mururoa (Polynésie Française): Académie des Sciences (Paris), Comptes Rendus, 316 (série II), p. 1485–1491.

Gautret, P., and Marin, F., 1993, Evaluation of diagenesis in scleractinian corals and calcified demosponges by substitution index measurement and intraskeletal organic matrix analysis: Courier Forschungsinstitut Senckenberg, v. 164, p. 317–327.

Gillikin, D.P., Lorrain, A., Navez, J., Taylor, J.W., André, L., Keppens, E., Baeyens, W., and Dehairs, F., 2005, Strong biological controls on Sr/Ca ratios in aragonitic marine bivalve shells: Geochemistry, Geophysics, Geosystems, 6, Q05009, doi: 10.1029/2004GC000874.

Glover, C.P., and Kidwell, S.M., 1993, Influence of organic matrix on the post-mortem destruction of molluscan shells: Journal of Geology, v. 101, p. 729–747.

Grossman, E.L., Mii, H.-S., Zhang, C., and Yancey, T.E., 1996, Chemical variation in Pennsylvanian brachiopod shells: Diagenetic, taxonomic, microstructural, and seasonal effects: Journal of Sedimentary Research, v. 66, p. 1011–1022.

Hare, P.E., and Abelson, P.H., 1965, Amino acid composition of some calcite proteins: Carnegie Institution of Washington Year Book, v. 64, p. 223–232.

Jablonski, D., Roy, K., Valentine, J.W., Price, R.M., and Anderson, P.S., 2003, The impact of the pull of the recent on the history of marine diversity: Science, v. 300, p. 1133–1135.

Jefferies, R.P.S., 1961, The Palaeontology of the Actinocamax Plenus Zone (Lowest Turonian) in the Anglo-Paris Basin: Palaeontology, v. 4, p. 609–647.

Kallend, J.S., Kocks, U.F., Rollett, A.D., and Wenk, H.R., 1991, Operational texture analysis: Materials Science and Engineering A, v. 132, p. 1–11.

Kennedy, W.J., Taylor, J.D., and Hall, A., 1969, Environmental and biological controls on bivalve shell mineralogy: Biological Reviews, v. 44, p. 499–530.

Kidwell, S.M., 1998, Time-averaging in the marine fossil record: Overview of strategies and uncertainties: Geobios, v. 30, p. 977–995.

Kidwell, S.M., and Bosence, D.W.J., 1991, Taphonomy and time-averaging of marine shelly faunas, *in* Allison, A., and Briggs, D.E.G., eds., Taphonomy: Releasing the data locked in the fossil record: Plenum, New York, p. 115–209.

Kidwell, S.M., and Flessa, K.W., 1995, The quality of the fossil record: Population, species and communities: Annual Review of Earth and Planetary Sciences, v. 24, p. 422–464.

Kowalewski, M., 1996, Time-averaging, overcompleteness, and the geological record: Journal of Geology, v. 104, p. 317–326.

Kowalewski, M., Flessa, K.W., and Hallman, D.P., 1995, Ternary taphograms: Triangular diagrams applied to taphonomic analysis: PALAIOS, v. 10, p. 478–483.

Krinsley, D., 1960, Magnesium, strontium and aragonite in the shells of certain littoral gastropods: Journal of Paleontology, v. 34, p. 774–775.

Lawrence, D.R., 1968, Taphonomy and information losses in fossil communities: Geological Society of American Bulletin, v. 79, p. 1315–1330.

Lézine, A.M., Saliége, J.F., Mathieu, R., Tagliatela, T.L., Mery, S., Charpentier, V., and Cleuziou, S., 2002, Mangroves of Oman during the late Holocene: Climatic implications and impact on human settlements: Vegetation History and Archaebotany, v. 11, p. 221–232.

Liang, Y., Zhao, J., Wang, L., and Li, F., 2008, The relationship between mechanical properties and crossed-lamellar structure of mollusk shells: Materials Science and Engineering A, v. 483–484, p. 309–312.

LOWENSTAM, H.A., 1961, Mineralogy, O^{18}/O^{16} ratios, and strontium and magnesium contents of recent and fossil brachiopods and their bearing on the history of the oceans: Journal of Geology, v. 69, p. 241–260.

MAGNANI, G., BARTOLOMEI, P., CAVULLI, F., ESPOSITO, M., MARINO, E.C., NERI, M., RIZZO, A., SCARUFFI, S., and TOSI, M., 2007, U-series and radio carbon dates on mollusc shells from the uppermost layer of the archaeological site of KHB-1, Ra's al Khabbah, Oman: Journal of Archaeological Science, v. 34, p. 749–755.

MELDAHL, K.H., and FLESSA, K.W., 1990, Taphonomic pathways and comparative biofacies and taphofacies in a recent intertidal/ shallow shelf environment: Lethaia v. 23, p. 43–60.

MORSÁN, E.M., 2000, Dinámica poblacional y explotación de la almeja púrpura, *Amiantis purpurata L.*: Unpublished Ph.D. dissertation, Universidad Nacional del Sur, Bahía Blanca, Argentina, 172 p.

MORSÁN, E.M., 2003, Spatial analysis and abundance estimation of the southernmost population of purple clam, *Amiantis purpurata* in Patagonia (Argentina): Journal of the Marine Biological Association of the United Kingdom, v. 83, p. 4241–4251.

MORSE, J.W., WANG, Q., and TSIO, M.Y., 1997, Influences of temperature and Mg:Ca ratio on $CaCO_3$ precipitates from seawater: Geology, v. 25, p. 85–87.

NAVARTE, M., GONZÁLEZ, R., and FILIPPO, P., 2007, Artisanal mollusk fisheries in San Matías Gulf (Patagonia, Argentina): An appraisal of the factors contributing to unsustainability: Fisheries Research, v. 87, p. 68–76.

NEVES, N.M., and MANO, J.F., 2005, Structure/mechanical behavior relationships in crossed-lamellar sea shells: Materials Science and Engineering C, v. 25, p. 113–118.

NILSEN, T.H., 1987, Stratigraphy and sedimentology of the Eocene Tejon Formation, western Techachapi and San Emigdio Mountains, California: United States Geological Survey Professional Paper, v. 1268, p. 1–110.

OKUMURA, M., and KITANO, Y., 1986, Coprecipitation of alkali metal ions with calcium carbonate: Geochimica et Cosmochimica Acta, v. 50, p. 49–58.

OLIVER, A., SOLÍS, C., RODRÍGUEZ-FERNÁNDEZ, L., and ANDRADE, E., 1996, Chemical diagenesis in fossil shells from Baja California, México, studied using PIXE and mass spectrometry: Nuclear Instruments and Methods in Physics Research B, v. 118, p. 414–417.

OLSZEWSKI, T.D., 1999, Taking advantage of time-averaging: Paleobiology, v. 25, p. 226–238.

OLSZEWSKI, T.D., 2004, Modeling the influence of taphonomic destruction, reworking, and burial on time-averaging in fossil accumulations: PALAIOS, v. 19, p. 39–50.

PANDOLFI, J.M., and GREENSTEIN B.J., 1997, Taphonomic alteration of reef corals: Effects of reef environment and coral growth form, I. The Great Barrier Reef: PALAIOS, v. 12, p. 27–42.

PASTORINO, G., 1989, Lista preliminar de moluscos cuaternarios de algunos yacimientos de Rio Negro y Chubut, Argentina: Comunicaciones de la Sociedad Malacológica del Uruguay, v. 7, p. 129–137.

PASTORINO, G., 2000, Asociaciones de moluscos de las terrazas marinas cuaternarias de Rio Negro y Chubut, Argentina: Ameghiniana, v. 37, p. 131–156.

PERRIN, C., 2004, Diagenèse précoce des biocristaux carbonatés: Transformations isominérales de l'aragonite corallienne: Société Géologique de France, Bulletin, v. 175, p. 95–106.

PERRIN, C., and CUIF, J.P., 2001, Ultrastructural controls on diagenetic patterns of scleractinian skeletons: Evidence at the scale of colony life-time: Tohoku University Museum Bulletin, v. 1, p. 210–218.

PERRIN, C., and SMITH, D.C., 2007, Earliest steps of diagenesis in living Scleractinian corals: Evidence from ultrastructural pattern and Raman spectroscopy: Journal of Sedimentary Research, v. 77, p. 495–507.

PILKEY, O.H., and GOODELL, H.G., 1964, Comparison of the composition of fossil and recent mollusk shells: Geological Society of America Bulletin, v. 75, p. 217–228.

PINGITORE, N.E.J., 1976, Vadose and phreatic diagenesis: Processes, products and their recognition in corals: Journal of Sedimentary Petrology, v. 46, p. 985–1006.

PINGITORE, N.E.J., MEITZNER, G., and LOVE, K., 1995, Identification of sulfate in natural carbonates by X-ray absorption spectroscopy: Geochimica et Cosmochimica Acta, v. 59, p. 2477–2483.

PIRRIE, D., and MARSHAL, J.D., 1990, Diagenesis of Inoceramus and Late Cretaceous paleoenvironmental geochemistry; a case study from James Ross Island, Antarctica: PALAIOS, v. 5, p. 336–345.

POKROY, B., FIERAMOSCA, J.S., VON DREELE, R.B., FITCH, A.N., CASPI, E.N., and ZOLOTOYABKO, E., 2007, Atomic structure of biogenic aragonite: Chemistry of Materials, v. 19, p. 3244–3251.

POPP, B.N., ANDERSON, T.F., and SANDBERG, P.A., 1986, Textural, elemental and isotopic variations among constituents in Middle Devonian limestones, North America: Journal of Sedimentary Petrology, v. 56, p. 715–727.

POWELL, M.G., and KOWALEWSKI, M., 2002, Increase in evenness and sampled alpha diversity through the Phanerozoic: Comparison of early Paleozoic and Cenozoic marine fossil assemblages: Geology, v. 30, p. 331

PURDY, E.G., 1968, Carbonate diagenesis: An environmental survey: Geologica Romana, v. 7, p. 183–228.

PURTON, L.M.A., SHIELDS, G.A., BRASIER, M.D., and GRIME, G.W., 1999, Metabolism controls Sr/Ca ratios in fossil aragonitic mollusks: Geology, v. 27, p. 1083–1086.

RAUP, D.M., and STANLEY, S.M., 1978, Principles of Paleontology, second edition: W.H. Freeman and Company, New York, 481 p.

RHOADS, D.C., and LUTZ, R.A., 1980, Skeletal growth of aquatic organisms. Biological records of environmental change: Plenum Press, New York and London, 750 p.

ROISNEL, T., and RODRÍGUEZ-CARVAJAL, J., 2008, FullProf, http://www.ill.eu/sites/fullprof/. Checked June 2013.

RUTTER, N., SCHNACK, E.J., DEL RIO, J., FASANO, J.L., ISLA, F.I., and RADTKE, U., 1989, Correlation and dating of Quaternary littoral zones along the Patagonian coast, Argentina: Quaternary Science Reviews, v. 8, p. 213–234.

RUTTER, N., RADKE, U., and SCHNACK, E.J., 1990, Comparison of ESR and amino acid data in correlating and dating Quaternary shorelines along the Patagonian Coast, Argentina: Journal of Coastal Research, v. 6, p. 391–411.

SANDBERG, P.A., and HUDSON, J.H., 1983, Aragonite relic preservation in Jurassic calcite-replaced bivalves: Sedimentology, v. 30, p. 879–892.

SCHÖNE, B.R., ZHANG, Z., JACOB, D., GILLIKIN, D.P., TÜTKEN, T., GARBE-SCHÖNBERG, D., MCCONNAUGHEY, T., and SOLDATI, A., 2010, Effect of organic matrices on the determination of the trace element chemistry (Mg, Sr, Mg/Ca, Sr/Ca) of aragonitic bivalve shells (*Arctica islandica*): Comparison of ICP-OES and LA-ICP-MS data: Geochemical Journal, v. 44, p. 23–37.

SHANNON, R.D., 1976, Revised effective ionic radii and systematic studies of interatomic distances in halides and chalcogenides: Acta Crystallographica A32, p. 751–767.

SPAETH, C.H.R., HOEFS, J., and VETTER, U., 1971, Paleotemperatures some aspects of isotopic composition of belemnites and related: Geological Society of America Bulletin, v. 82, p. 3139–3150.

STEHLI, F.G., and HOWER, J., 1961, Mineralogy and early diagenesis of carbonate sediments: Journal of Sedimentary Petrology, v. 31, p. 358–371.

TANTANASIRIWONG, R., 1979, A checklist of marine bivalves from Phuket Island, adjacent mainland and offshore western peninsular Thailand: Phuket Marine Biological Center, Research Bulletin, v. 27, p. 1–15.

TONG, H., HU, J., MA, W., ZHONG, G., YAO, S., and CAO, N., 2002, *In situ* analysis of the organic framework in the prismatic layer of mollusc shell: Biomaterials, v. 23, p. 2593–2598.

VAN DER MEIDE, P.H., WESTBROEK, P., DE JONG, E.W., DE LEEUW, J.W., and MEUZELAAR, H.L.C., 1980, Characterization of macromolecules from fossil shells by immunology and Curie-Point pyrolysis Mass Spectrometry, *in* Omori, M., and Watabe, N., eds., The Mechanisms of Biomineralization in Animals and Plants: Tokai University Press, Tokyo, p. 251–256.

VEIZER, J., 1983, Trace elements and isotopes in sedimentary carbonates: Reviews in Mineralogy, v. 11, p. 265–300.

WAINWRIGHT, S.A., 1969, Stress and design in bivalve mollusk shell: Nature, v. 224, p. 777–779.

WEBB, G.E., PRICE, G.J., NOTHDURFT, L.D., DEER, L. and RINTOUL, L., 2007, Cryptic meteoric diagenesis in freshwater bivalves: Implications for radiocarbon dating, Geology, v. 35, p. 803–806.

YANG, W., KASHANI, N., LI, X.-W., ZHANG, G.-P., and MEYERS, M.A., 2011a, Structural characterization and mechanical behavior of a bivalve shell (*Saxidomus purpuratus*): Materials Science and Engineering C, v. 31, p. 724–729.

YANG, W., ZHANG, W., LIU, H., and LI, X., 2011b, Microstructural Characterization and Hardness Behavior of a Biological *Saxidomus purpuratus* Shell: Journal of Material Science and Technology, v. 27, p. 139–146.

ZHANG, Z., 2009, Geochemical properties of shells of *Arctica islandica* (Bivalvia): Implications for environmental and climatic change: Ph.D. dissertation, Geographie der Goethe-Universität in Frankfurt, Frankfurt, 123 p.

ZHOU, W., HEAD, M.J., WANG, F., DONAHUE, D.J., and JULL, A.J.T., 1999, The reliability of AMS radiocarbon dating of shells from China: Radiocarbon, v. 41, p. 17–24.

ZUSCHIN, M., and STANTON, R.J., JR., 2001, Experimental measurement of shell strength and its taphonomic interpretation: PALAIOS, v. 16, p. 161–170.

ACCEPTED JUNE 25, 2013